Seasonal dynamics of phytoplankton and bacterioplankton at the ultra-oligotrophic southeastern Mediterranean Sea

Tom Reich[1], Tal Ben-Ezra[1,2], Natalya Belkin[3], Anat Tsemel[1,2], Dikla Aharonovich[1], Dalit Roth-Rosenberg[1], Shira Givati[1], Or Bialik[4], Barak Herut[3,4], Ilana Berman-Frank[1], Miguel Frada[5,6], Michael D. Krom[1,2], Yoav Lehahn[4], Eyal Rahav[3]* and Daniel Sher[1]*

[1]Department of Marine Biology, Leon H. Charney School of Marine Sciences, University of Haifa, Israel; [2]Morris Kahn Marine Research Station, Leon H. Charney School of Marine Science, University of Haifa, Haifa, 3498838, Israel. [3]Israel Oceanographic and Limnological Research, Haifa, Israel. [4]Department of Maritime Geosciences, Leon H. Charney School of Marine Sciences, University of Haifa, Israel. [5]The Interuniversity Institute for Marine Sciences in Eilat, POB 469, 88103 Eilat, Israel. [6]Dept. of Ecology, Evolution and Behavior – Alexander Silberman Institute of Life Sciences, Hebrew University of Jerusalem, Jerusalem 91904, Israel

*Corresponding authors:

dsher@univ.haifa.ac.il

eyal.rahav@ocean.org.il

Keywords: Eastern Mediterranean, Levantine Basin, seasonal dynamics, primary productivity, bacterial productivity, phytoplankton, *Prochlorococcus*, *Synechococcus*, pico-eukaryotes.

Highlights

- Bacterioplankton dynamics were assessed monthly in the Eastern Mediterranean Sea
- Small-sized picophytoplankton numerically dominated the phytoplankton community
- Seasonal phytoplankton dynamics are similar to BATS and Red Sea, but not ALOHA
- Annual primary productivity is among the lowest in the world's oceans
- Bacterial to primary production ratio is higher than most oligotrophic seas

Abstract

The Eastern Mediterranean Sea (EMS) is an ultra-oligotrophic, enclosed basin strongly impacted by regional and global anthropogenic stressors. Here, we describe the annual (2018-19) dynamics of phyto- and bacterioplankton (abundances, pigments and productivity) in relation to the physical and chemical conditions in the photic water column at the offshore EMS water (Station THEMO-2, ~1,500m depth, 50km offshore). Annual patterns in phytoplankton biomass (as chlorophyll a), primary and bacterial productivity differed between the mixed winter (January-April) and the thermally stratified (May-December) periods. *Prochlorococcus* and *Synechococcus* numerically dominated the picophytoplankton populations, with each clade revealing different temporal and depth patterns, while pico-eukaryotes (primarily haptophytes) were less abundant, yet likely contributed significant biomass. Integrated primary productivity (~32 gC m^{-2} y^{-1}) was lower compared with other well-studied oligotrophic locations, including the north Atlantic and Pacific (HOT and BATS observatories), the western Mediterranean (DYFAMED observatory) and the Red Sea, and was on-par with the ultra-oligotrophic South Pacific Gyre. In contrast, integrated bacterial production (~11 gC m^{-2} y^{-1}) was similar to other oligotrophic locations. Phytoplankton seasonal dynamics were reminiscent of those at BATS and the Red Sea, suggesting an observable effect of winter mixing in this ultra-oligotrophic location. These results highlight the ultra-oligotrophic conditions in the EMS and provide, for the first time in this region, a full-year baseline and context to ocean observatories in the region.

1 Introduction

Convective mixing of the water column is one of the main mechanisms responsible for transport of nutrients to the photic zone of oligotrophic oceans and seas, often resulting in increased phytoplankton biomass and activity (Behrenfeld 2010; Williams et al. 2013). This process usually occurs during wintertime upon the progressive cooling of the sea surface, although other mechanisms may also deliver nutrients to the mixed layer such as physical upwelling along shorelines, frontal systems and gyres (Anabalón et al. 2016; Groom et al. 2005), nutrient runoff from rivers (Jickells 1998), and atmospheric deposition (Guieu et al. 2014). As stratification is established during springtime, nutrients gradually become depleted, which, together with other processes such as increased predation, lead to a decline in algal biomass and productivity (Behrenfeld and Boss 2014). This cycle has been extensively studied over decades in the major oligotrophic gyres (e.g. HOT and BATS) (Steinberg et al. 2001), as well in other locations including the Western Mediterranean and Red Seas (Genin et al. 2018; Marty and Chiavérini 2010; Marty et al. 2002), and is considered a fundamental driving force of marine ecosystem structure and function.

The Mediterranean Sea is a small basin surrounded by land and yet it is ultra-oligotrophic (Berman-Frank and Rahav 2012; Siokou-Frangou et al. 2010). The oligotrophic nature of this system, and especially of the Eastern Mediterranean Sea (EMS), is mainly driven by its general anti-estuarine circulation (Pinardi and Masetti 2000; Tanhua et al. 2013; Zervakis and Georgopoulos 2002). Additionally, the relatively stable density stratification throughout most of the year (winter mixing rarely exceeds the 200 m depth, (Brenner et al. 1991; d'Ortenzio et al. 2005)) has been suggested to result in a very low supply of deep water nutrients to the euphotic zone (Hazan et al. 2018a; Tanhua et al. 2013). Finally, modern riverine inputs into the EMS are extremely low, especially since the Nile was dammed in the 1960s, (Krom et al. 2014). The abovementioned conditions makes the EMS, and specifically

the easternmost Levantine basin, among the warmest, saltiest and least productive waters in the world (Kress et al. 2014; Ozer et al. 2017; Psarra et al. 2000).

Despite the importance of the EMS coastline in providing ecosystem services to over 70 million people e.g. (Peled et al. 2018), it lacks the continued high resolution records available from other oligotrophic regions such as the North Atlantic (the Bermuda Atlantic Time Series, BATS), North Pacific (The Hawaii Ocean Time-Series station ALOHA), the Western Mediterranean e.g. station DYFAMED (Marty and Chiavérini 2010; Marty et al. 2002) and, to a lesser extent, the Red Sea (e.g. (Shaked and Genin 2017). Specifically, detailed phytoplankton and bacterioplankton time-series are missing, and are important in order to both understand the current system and the ways it may be impacted by local, regional and global change (e.g. (Kim et al. 2019; Marty and Chiavérini 2010). Thus, studying the dynamics of the microorganisms at the base of the marine food-web over time are of great ecological importance.

Studies from the early 1980's showed a clear seasonal cycle of chlorophyll a (an indirect proxy of algal biomass) and primary production in surface waters of both neritic and pelagic locations, with the changes attributed primarily to picophytoplankton (Azov 1986; Berman et al. 1984; Kimor and Wood 1975; Yacobi et al. 1995). More recent studies of the EMS show similar seasonal trends using remote-sensing of surface chlorophyll a (Rosenberg et al. 2020) and in measurements of cell numbers, production and dinitrogen fixation in coastal waters (Rahav et al. 2018; Raveh et al. 2015). However, to the best of our knowledge, no detailed temporal (monthly) measurements have been presented of microbial processes and phytoplankton community structure at the offshore EMS waters. In this study, we followed the composition and activity of phytoplankton and bacterioplankton from station THEMO-2 in the offshore EMS over a full year at monthly temporal resolution, and at high depth resolution (~20 samples, ~12 of them across the photic zone). These measurements were

performed as part of the SoMMoS (Southeastern Mediterranean Monthly cruise Series) campaign, which compared an open-ocean station with one at the edge of the continental shelf (Figure 1A). Additional studies from this cruise series will focus on the carbonate system (Juntao et al. *in prep*), nutrient dynamics (Ben Ezra et al. *submitted*), coccolithophore dynamics (Keuter et al. *in prep*) and a detailed comparison of the offshore and coastal stations (Krom et al. *in prep*). Together, these studies provide a baseline allowing the interpretation of two long-term ocean observatories recently established in the EMS: the DeepLev (Katz et al. 2020) and THEMO (Diamant et al. 2020), as well as comparison to long-term monitoring activities (Ozer et al. 2017; Rahav et al. 2019; Sisma-Ventura et al. 2021).

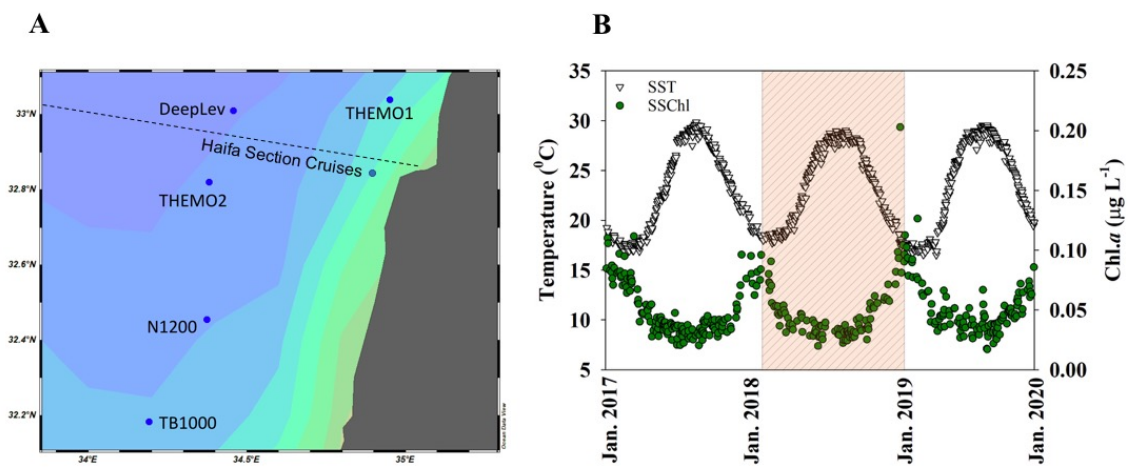

Figure 1: Overview of the SoMMoS sampling locations context. A) A map of the Levantine Basin (EMS) showing the location of the THEMO-2 sampling site (the focus of this study), as well as of additional observatories and locations of long-term studies discussed here: THEMO-1, DeepLev (Katz et al. 2020), N-1200 (Rosenberg et al. 2020), TB-1000 (Yogev et al. 2011) and the Haifa section transect cruises (Kress et al. 2014; Ozer et al. 2017). B) Changes in satellite-derived sea surface temperature (orange) and sea surface chlorophyll a (green) from the 1 km^2 region surrounding THEMO-2 between 2017-2020.

Data were extracted from the Copernicus Marine Environment Monitoring Service (CMEMS, https://marine.copernicus.eu/). The period of this study is shaded.

2 Materials and Methods

2.1 Cruises and sample collection

Water samples were collected as part of the SoMMoS project during twelve cruises, from February 2018 until January 2019. Each expedition took samples at two stations: THEMO2, an open ocean station at a depth of ~1500 m (~50 Km from the coast, 32.820 N, 34.380 E), and THEMO1 which is positioned at the edge of the continental shelf at ~125m depth (~10 Km from the coast, 33.040 N, 34.950 E). THEMO2 was sampled from 12:00-22:00, while THEMO1 was sampled during the night (typically 00:00-02:00). Here, we will present information from data collected at the offshore THEMO2 station. Samples were collected using a 12-bottle rosette with 8 L Niskin bottles. Samples were collected at 20-24 depths across the entire water column (11-12 bottles between the surface and 200 m, which we define here as the photic zone). Sampling depths were selected based on real-time data of Conductivity, Temperature, Depth (CTD) profiler (Seabird 19 Plus), an oxygen optode (on some cruises) and a fluorescence meter (Turner designs, Cyclops-7). The continuous data was processed using the Sea-Bird data conversion software, and minimized using bin averaging. One bin of data lines was defined as a change of 1 decibar (db) between each bin. The first two meters of measurements were compiled together to account for sensors and CTD pump adjustment time and rosette depth while at sea surface. Each cast allocated water for analysis in the following order to give priority to the more 'sensitive' parameters: dissolved methane, pH, alkalinity, dissolved inorganic carbon, inorganic nutrients, total and dissolved organic carbon, cell count, primary and bacterial production, DNA and algal pigment markers. A summary of all of the currently-available measurements can be found in Supplementary Table S1, and the BCO-DMO (BCO-DMO acronym HAD-FBA) and ISRAMAR (https://isramar.ocean.org.il/isramar2009/) databases. Mixed layer depth (MLD) was calculated using a temperature difference of Δ0.3 °C (Mena et al. 2019). Calculations based

on a density difference of $\Delta 0.15$ kg/m^3 yielded similar results. During several months (February-April 2018 and January 2019), the density plots revealed a progressive increase in density without a clear pycnocline but with multiple "bumps", indicative of water column instability down to below 200 m (Supplementary Figure S1). At these times, the MLD calculations based on a defined difference in temperature or salinity from the surface preclude a robust estimate of the mixed layer depth, as they may underestimate the actual values. Based on these calculations, we divide the study period into 'a generally mixed period' during January-April (winter/spring), and a 'stratified period' during May-December (summer/autumn, Table 1). Estimates based on the vertical distribution of inorganic nutrient concentrations suggest the mixing period may have begun as early as November 2018 (T. Ben-Ezra et al. *submitted*.). We note that the monthly sampling resolution likely to 'miss' short-lived deep mixing events, as can be observed from mooring operations (e.g. (Gunn et al. 2020).

2.2 Bacterial and primary productivity

Heterotrophic prokaryotic productivity (hereafter referred to as bacterial productivity, BP) was estimated using the ^{3}H-leucine incorporation method (Simon and Azam 1989; Smith and Azam 1992). Triplicate 1.7ml of ocean water were taken from each sampled depth and incubated with ^{3}H-leucine (100 nmol leucine L^{-1}) for 4h at room temperature in the dark immediately after sampling. After incubation, incorporation was terminated by adding 100 µl trichloroacetic acid (TCA). As a negative control for non-specific binding, another set of triplicates were sampled from a surface layer and treated with TCA immediately after the addition of the radioactive tracer. At the end of each cruise, the samples were processes using the micro-centrifugation protocol (Simon and Azam 1989) and 1ml scintillation cocktail

(ULTIMA-GOLD) was added to all samples before counted using TRI-CARB 2100 TR (PACKARD) scintillation counter.

Photosynthetic carbon fixation rates were estimated using the ^{14}C incorporation method (Nielsen 1952), with several modifications (Hazan et al. 2018a). Triplicate 50 ml samples were taken from each depth within the photic zone and from one aphotic depth and kept at surface light and temperature conditions. The 'dark' sample served as blank and was kept under the same temperature as the 'light' samples. Radioactive spiking was done at ~08:00 AM the day following of the cruise in order to start a 24h incubation for all samples (including those collected at THEMO-1 station, not shown) at the same time. Samples were spiked with 50µl (5 µCi) of $NaH^{14}CO_3$ tracer and were incubated for 24 h under 3 light regimes: surface illumination (samples from the upper mixing depths), 50% illumination (samples from below the mixing depth to the DCM) and ~1% illumination (samples from the DCM and below). Shading was performed using neutral density nets, thus changing light intensity but not spectral properties. Water samples were then filtered through GF/F filters (0.7 µm nominal pore size, 25 mm diameter) using low vacuum pressure (< 50 mmHg) and rinsed 3 times with filtered sea water. Filters from each sample were then put in scintillation vials where 50 µl of 32%HCl solution was immediately added in order to remove excess ^{14}C-bicarbonate and kept overnight for incubation. After incubation 5 mL scintillation cocktail (ULTIMA-GOLD) was added to the samples and counted using TRI-CARB 2100 TR (PACKARD) scintillation counter. Three random aliquots were counted immediately after the addition of the radiotracer (without incubation) with ethanolamine to serve as added activity measurements.

2.3 Picophytoplankton abundance using flow-cytometry

Triplicates water samples (1.5 ml) were collected from each sampling depth, put in cryo-vials (Nunc), and supplemented with 7.5 µl 25% glutaraldehyde (Sigma). Vials were incubated in the dark for 10 min, flash-frozen in liquid nitrogen, and stored in -80 ^{o}C freezer. Before analysis, samples were thawed in the dark at room temperature. Each sample was run twice on a BD Canto II flow-cytometer with 2 µm diameter fluorescent beads (Polysciences, Warminster, PA, USA) as a size and fluorescence standard. In the first run three types of phytoplankton cells were identified based on their natural auto-fluorescence: *Prochlorococcus*, *Synechococcus* and picoeukaryotes. Cells were differentiated based on cell chlorophyll (Ex482nm/Em676nm, PerCP channel) and phycoerythrin fluorescence (Ex564nm/Em574nm), and by the size of cell (forward scatter). Before the second FCM, run samples were stained with SYBR Green I (Molecular Probes/ ThermoFisher) to enable counting followed by detection at Ex494nm/Em520nm (FITC channel). This provided counts of the total bacterial population (phytoplankton + heterotrophic bacteria and archaea) as well as a distinction between cells with High or Low DNA content (not shown). Data were processed using FlowJo software. Flow rates were determined several times during each running session by weighing tubes with double-distilled water, and counts of the standard beads were used to verify a consistent flow rate.

2.4 Algal pigment markers

Eight litters of seawater were collected from all photic sample depths and one from a dark depth (depth varies between cruises). Water was filtered onto GF/F filters (0.7 µm nominal pore size, 47mm diameter, Waters) using a peristaltic pump until either all 8 L were filtered or the filter became blocked, in which case the volume filtered was recorded. Filters were placed in cryo-vials and flash frozen in liquid nitrogen until they could be stored in a -80 ^{o}C

freezer. Pigments were extracted in 1ml 100% methanol for 3 h at room temperature and clarified using syringe filters (Acrodisc CR, 13 mm, 0.2 μm PTFE membranes, Pall Life Sciences). Total chlorophyll was measured spectrophotometrically using a NanoDrop 2000c (Thermo Sciences) at 632, 652, 665 and 695 nm, and the concentration of chlorophyll a was calculated (Ritchie 2008). Ultra high-pressure Liquid Chromatography (UPLC) was performed on an ACQUITY UPLC system (Waters) equipped with a photodiode array detector. A C8 column (1.7 μm particle size, 2.1 mm internal diameter, 50 mm column length, ACQUITY UPLC BEH, 186002877) was used. The chromatography method was adapted for UPLC from the LOV method (Hooker 2005). Samples were preheated to 30 °C and column to 50 °C before each run. Running buffers were a 70:30 mixture of methanol and 0.5M ammonium acetate (buffer A) and 100% methanol (buffer B). The program consisted of an isocratic run using a 80:20 mixture of buffers A:B for 2min, followed by a linear gradient to 50:50 for 7 minutes and an increase to 100% solvent B. The flow rate was 0.5ml/min. Pigment standards from DHI (Denmark) were used to identify the UPLC peaks (chlorophyll a, divinyl-chlorophyll a, chlorophyll b, chlorophyll c2, zeaxanthin, beta-carotene, diatoxanthin, fucoxanthin, peridinin, 19’- butanoyloxyfucoxanthin and 19’-hexanoyloxyfucoxanthin). Due to potential degradation of the pigment standards, we present the total chlorophyll measured spectrophotometrically and the pigment ratios within each UPLC run.

3 Results

3.1 Physical and chemical properties of the water column

Between January 2016 and December 2019, a clear pattern was observed in satellite-derived sea surface temperature at the THEMO-2 location (Figure 1B), which was mirrored during the monthly cruise measurements (February 2018-January 2019, Figure 2A). The measured

in-situ sea surface temperatures increased by > 11°C from the winter minimum of ~17.9 °C to the summer maximum of 29.1 °C (Figure 2A, Supplementary Figure S2, Table 1). Sea surface salinity also increased from a winter minimum of ~39.3 psu to a summer maximum of 39.8 psu (Figure 2B, Supplementary Figure S2). Both temperature and salinity minima were higher than the climatological minima (~15.2 °C and 38.9 psu, measured between 2002-2020, (Herut and Rahav 2019), suggesting that the sampling period represents a relatively warm and salty year. The temporal changes in sea surface temperature and salinity led to differences in the water density profiles (Figure S1), indicative of stratification of the upper water layer between May and December 2018 (Mixed Layer Depth = 15-49 meters) and mixed between February-April 2018 and January 2019 (MLD not determined, see materials and methods) (Table 1). Inorganic nutrient (NO_3+NO_2) concentrations began to increase in the mixed layer already during November, suggesting that the stratification had started to erode earlier than observed based on the density profiles, possibly due to short-term mixing events (e.g. (Gunn et al. 2020).

Dissolved oxygen concentrations were at or above 100% saturation throughout the whole photic layer (0-200 m), ranging from ~180 µmol L^{-1} to ~240 µmol L^{-1} (Figure 2C). Soluble reactive phosphorus (SRP) concentrations at the surface water were at or close to the limit of detection ~0.006 μM, (~6 nM) throughout the year, whereas nitrate+nitrite (NOx) were close to the detection limits from August to November (limit of detection 0.013 μM) but reached 0.3-0.5 μM during the mixed period (Table 1, and see Ben Ezra et al. *submitted* for more information). The change in dissolved inorganic N and P suggest an excess of dissolved inorganic nitrogen compared to phosphorus during the mixed period if considering a 'typical' Redfield stoichiometry of 16:1 (Redfield 1934).

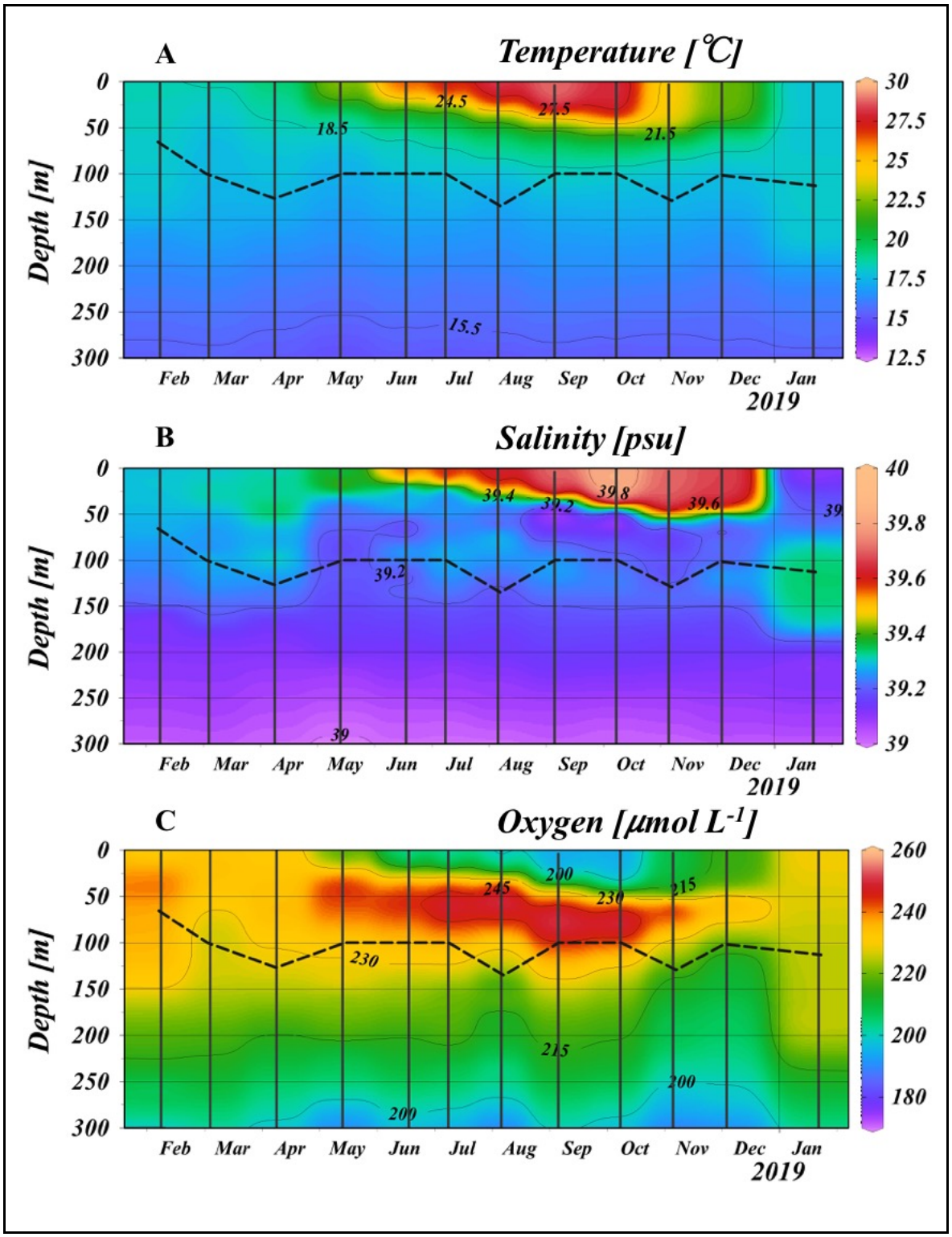
A
Temperature [℃]
Depth [m]
0
50
100
150
200
250
300
24.5
27.5
18.5
21.5
15.5
30
27.5
25
22.5
20
17.5
15
12.5
Feb
Mar
Apr
May
Jun
Jul
Aug
Sep
Oct
Nov
Dec
Jan
2019
B
Salinity [psu]
39.4
39.2
39.8
39.6
39.2
39
40
39.8
39.6
39.4
39.2
39
C
Oxygen [μmol L-1]
200
245
230
215
230
215
200
200
260
240
220
200
180

Figure 2: Temperature (A), Salinity (B) and oxygen concentrations (C) at THEMO2 station measured monthly between February 2018 to January 2019. The dashed line represents the depth of the Deep Chlorophyll Maximum (DCM). See Supplementary Figure S2 for the full depth profiles to ~1,400m.

Table 1: Median and range of major measured oceanographic parameters during the mixed and stratified periods. BDL – Below detection limit. ND – not determined (see materials and methods and Supplementary Figure S1 for details). Depth-integrated values are from 0-200m.

Parameter	**Mixed period (Jan-Apr)**	**Thermally Stratified period (May-Dec)**
SST (°C)	18.6 (17.9-19.6)	24.2 (22.1-29.1)
Mixed layer depth (m)	ND	26.5 (15-49)
DCM depth (m)	105 (67-125)	100 (100-135)
Surface (10 m) PO_4 [μM]	BDL (≤0.006 μM)	BDL (≤0.006 μM)
Surface (10 m) NOx [μM]	0.35 (0.29-0.58)	0.15 (0.03-0.54)
Surface Si [μM]	0.84 (0.8-1.04)	0.72 (0.58-1.04)
Chl *a* [mg m^{-2}]	14.58 (17.77-8.58)	8.81 (24.57-5.39)
Synechococcus [cells m^{-2}]	$1.04x10^{12}$ ($1.56x10^{12}$-$5.85x10^{11}$)	$5.03x10^{11}$ ($4.96x10^{10}$-$8.48x10^{11}$)
Prochlorococcus [cells m^{-2}]	$7.13x10^{11}$ ($2.5x10^{11}$-$2.2x10^{12}$)	$2.34x10^{12}$ ($1.02x10^{12}$-$3.2x10^{12}$)
Pico-eukaryotes [cells m^{-2}]	$1.73x10^{11}$ (0-$7.67x10^{11}$)	$8.65x10^{9}$ ($7.23x10^{7}$-$2.32x10^{11}$)
Heterotrophic prokaryotes [cells m^{-2}]	$6.65x10^{13}$ ($5.94x10^{13}$-$1.03x10^{14}$)	$5.42\ x10^{13}$ ($3.15x10^{13}$-$1.14x10^{14}$)
PP [mgC m^{-2} d^{-1}]	113 (68.8-142)	60.3 (47.8-111)

BP [mgC m^{-2} d^{-1}]	54.1 (31.6-70.6)	18.5 (6.7-26.8)

3.2 Chlorophyll a, Primary Productivity and Bacterial Productivity

While satellite-derived sea surface chlorophyll *a* showed a clear seasonal cycle over three years, with lower levels during the stratified period (Figure 1B), the entire photic zone displayed a more complex pattern (Figure 3A, B). A prominent Deep Chlorophyll Maximum (DCM) was observed year-round, ranging from depths of 60 m (February 2019) to 120 m (April 2019). The concentration of total chlorophyll a at the DCM was always higher than that measured at the surface, and ranged between ~0.15 μg L^{-1} during February-July, decreasing to ~0.07 μg L^{-1} during August-November. These values are within the range or somewhat lower than those measured in other studies in the EMS (~0.09-0.42 μg L^{-1}) (Christaki et al. 2001; Kress et al. 2014; Yacobi et al. 1995), and are ~2-5 fold lower than at BATS (Steinberg et al. 2001). Due primarily to the changes in the DCM, the integrated chlorophyll did not follow the same seasonal pattern as observed with the sea-surface satellites measurements (Figure 1B).

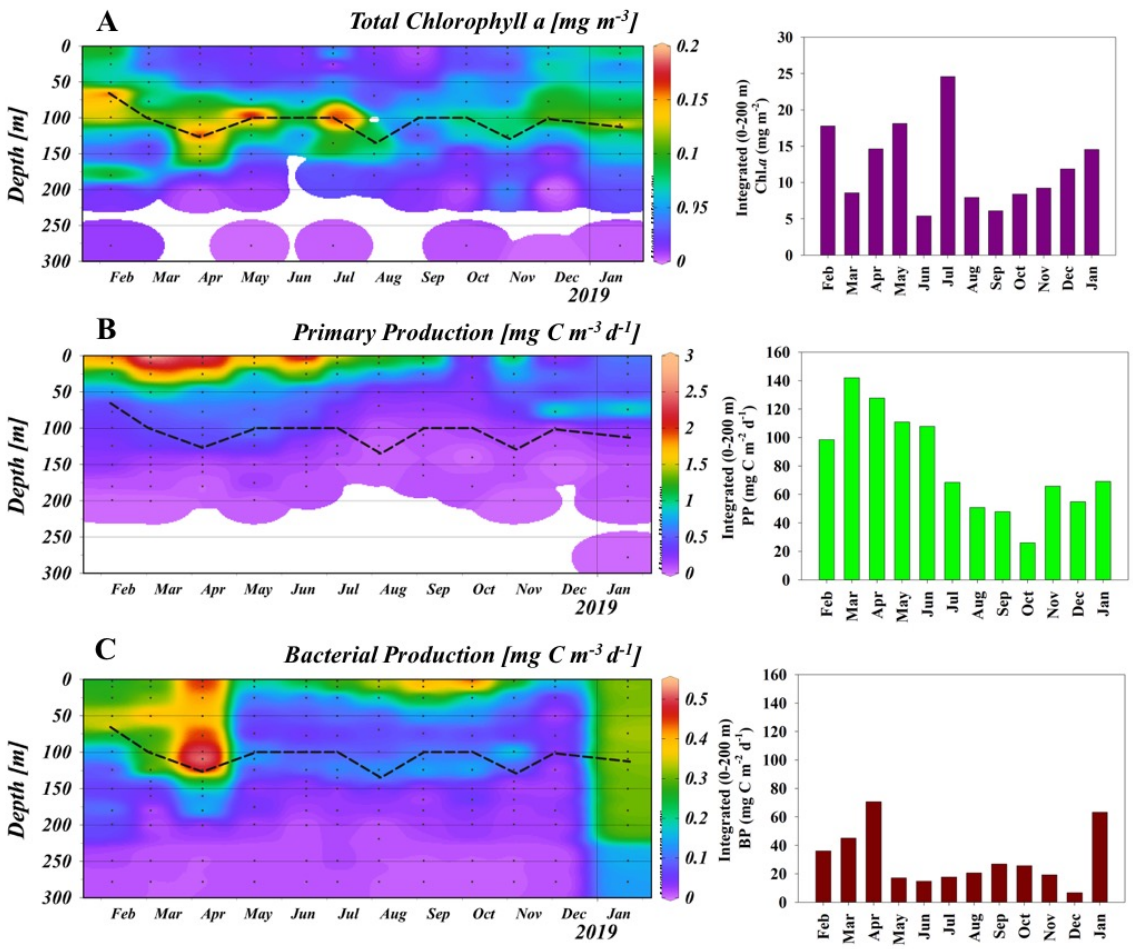

Figure 3: Seasonal changes in depth-resolved (left panels) and depth-integrated (right panels) chlorophyll *a* (A), primary productivity (B) and bacterial productivity (C). Black dots in panels A-C represent sampling points from each cruise. See Supplementary Figure S3 for the full depth profile of BP to ~1,400m.

Primary productivity (PP) was highest at the surface most of the year (1-3 mg C m^{-3} d^{-1}), declining with depth, with no observable maximum during most of the year at the DCM (0.08-0.47 mg C m^{-3} d^{-1}, Figure 3B). This is consistent with the chlorophyll maximum in ultra-oligotrophic oceans being decoupled from the PP maximum (Signorini et al. 2015). An exception to this pattern was observed during December 2019 and January 2020, where a

peak of PP was observed at around 75 m (0.93-0.96 mg C m^{-3} d^{-1}), slightly above the DCM (Figure 3B). The observed values at the surface are within the range or somewhat lower than previously measured values in the EMS (typically around ~2 mg C m^{-3} day^{-1}, but with values as high as ~18 mg C m^{-3} day^{-1} recorded), (Avnaim-Katav et al. 2020; Hazan et al. 2018a; Rahav et al. 2013a). The integrated PP values ranged between 69-142 mg C m^{-2} d^{-1} during the mixing period, and from 48 to 113 mg C m^{-2} d^{-1} during the stratified months (Figure 3B). These values are within the ranges observed in other studies of this region (reviewed in (Berman-Frank and Rahav 2012; Siokou-Frangou et al. 2010) and discussed below). Our measurements result in an annual PP of ~32 gC m^{-2}, which is lower by ~50% than most estimates from the EMS (Boldrin et al. 2002; Psarra et al. 2000). These annual estimates highlight the ultra-oligotrophic characteristics of the easternmost Levantine Basin.

During most of the year BP was highest at the surface (~0.2-0.5 mg C m^{-3} d^{-1}, Figure 3C, Supplementary Figure S3), within the range of previous observations at this area (Rahav et al. 2019; Tanaka et al. 2007; Van Wambeke et al. 2000). However, BP differed from PP in several aspects. First, a significant increase in BP was observed during April, with the highest rate observed at ~110 m where the DCM was detected. Indeed, a smaller secondary peak in BP was observed at a depth corresponding to the DCM throughout the year (Figure 3C). Second, surface BP increased during summer from a minimum in May to a maximum in September-October, before decreasing again. Third, during January 2019 a large increase was observed in BP, which was more-or-less homogenously distributed throughout the water column down to ~200 m. Depth-integrated BP ranged from a maximum of ~70 mg C m^{-2} d^{-1} during April 2018 and January 2019 to a minimum of ~20 mg C m^{-2} d^{-1} during May-December 2018, within the range of previous measurements ~10-45 mg C m^{-2} day^{-1} (e.g. (Christaki et al. 2011; Robarts et al. 1996; Van Wambeke et al. 2000). The integrated PP to

BP ratio also differed between the mixed and stratified periods. Where, during the mixed season the PP:BP ratio was ~3:1, while during the stratified period it reached ~5:1.

3.3 Phytoplankton abundance and specific functional groups

Picocyanobacteria (*Prochlorococcus* and *Synechococcus*) were the most abundant picophytoplankton cells throughout the year (Figure 4, Supplementary Figure S4). *Prochlorococcus* was more abundant during the stratified period, and predominated below the mixed layer (Figure 4A). Based on the ratio of divinyll chlorophyll a to total chlorophyll a (Figure 5A), *Prochlorococcus* contributed up to ~45% of the total phytoplankton biomass at the DCM during late fall (Figure 5A). *Synechococcus* was more abundant during the mixed period and in the surface waters (Figure 4B). Pico-eukaryotes were present at up to 10^4 cells ml^{-1} during February-June (Figure 4C), but there was no clear group-specific signal in the tested photosynthetic pigments during this period (Figure 5B-D), and thus the specific pico-eukaryotic groups present at this time could not be identified. In contrast, the presence of 19-hexanoyloxyfucoxanthin and 19-butanoyloxyfucoxanthin (19-Hex+19-But), primarily during August to November (Figure 5B), suggests the presence of haptophytes, and this was corroborated with microscopic identification of coccolithophores (see a more detailed discussion in Keuter et al, *in prep*). Finally, peridinin and fucoxanthin peaked during January, suggesting the presence of dinoflagellates and diatoms, respectively (Figure 5C,D).

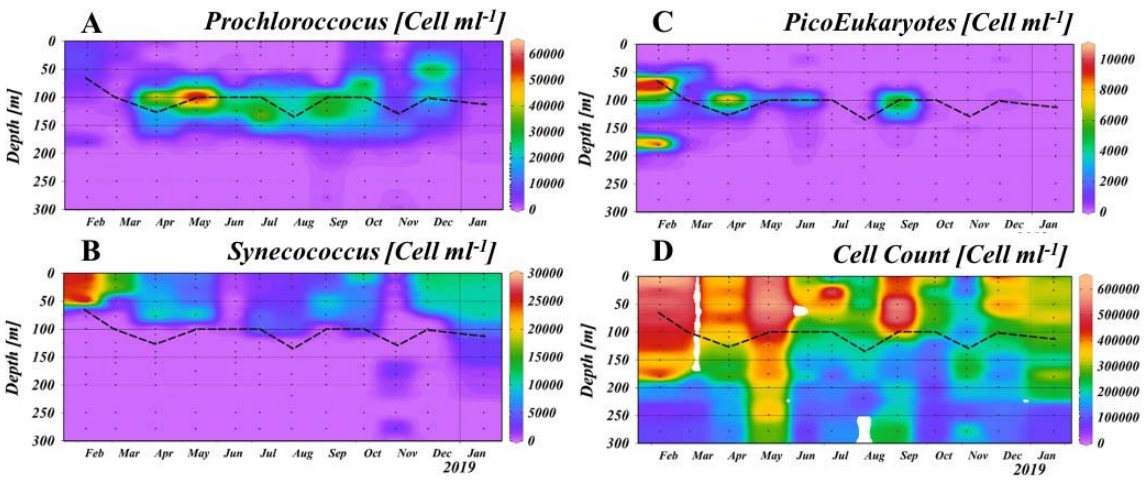

Figure 4: Annual dynamics of monthly measured picophytoplankton and bacterioplankton abundance: *Prochlorococcus* (A), *Synechococcus* (B), PicoEukaryotes (C) and total microbial counts (Sybr-stained, panel D) at the THEMO2 station. Black dots represent sample point from each cruise. No data were available from the March cruise for total microbial counts. Note the differences in the color scale for each plot. Dashed line represents the DCM. See Supplementary Figure S4 for the full depth profiles to ~1,400m.

Throughout the year, total prokaryotic microbial counts (Sybr-stained cells, thus including cyanobacteria, heterotrophic bacteria and archaea) ranged between 3 $x10^5$ to $6x10^5$ cells ml^{-1}, with higher values observed during February and May (Figure 4D). Heterotrophic bacteria were much more abundant than the combined phototrophs, the latter forming 2.4-8.5% of the total Sybr-stained cell counts. Below the photic layer, cell counts were typically lower, ranging from $1.9x10^4$-$4.5x10^5$ cells ml^{-1} (Supplementary Figure S4).

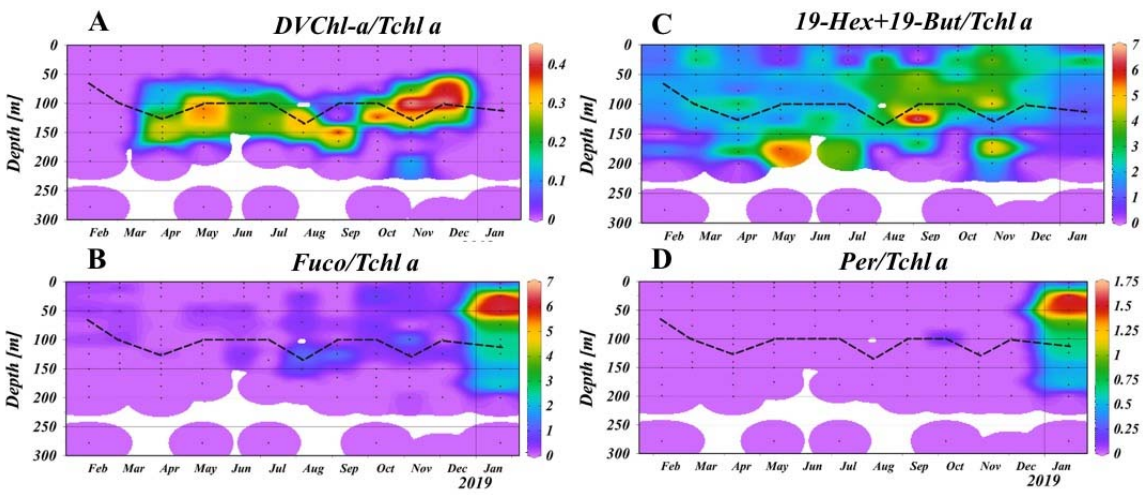

Figure 5: Monthly changes in the ratios ofmajor accessory pigments to Total chlorophyll *a*. A) divinyl chlorophyll *a* (DVChl-a). B) Combined 19-hexanoyloxyfucoxanthin and 19-butanoyloxyfucoxanthin (19-Hex+19-But). C) Fucoxanthin (Fuco). D) Peridinin. Black dots represent sampling depths. Dashed line represents the DCM.

4 Discussion

This study focuses on the seasonal dynamics of microbial productivity and of the major groups of phyto- and bacterio-plankton in the photic zone of the offshore EMS. The resulting dataset represents a monthly composite of corresponding physical, chemical, and biological measurements from the offshore EMS. Such relatively high-resolution *in-situ* measurements can provide a platform to integrate continuous physiochemical measurements from gliders and ocean observatories (THEMO and DeepLev, (Alkalay et al. 2020; Avnaim-Katav et al. 2020; Katz et al. 2020), as well as for biochemical and ecological models. We first compare the absolute values and temporal dynamics of primary and bacterial productivity between the EMS and other Low Nutrients Low Chlorophyll (LNLC) regions such as the North Atlantic and Pacific (HOT and BATS time-series, respectively) as well as the Red Sea. We then examine whether the observed temporal dynamics of the EMS picophytoplankton populations

can help identify similarities and differences between LNLC locations. Finally, we discuss the caveats of the current study, and suggest ways to improve our understanding of the dynamics of the EMS.

4.1 How oligotrophic is the EMS compared to other oligotrophic oceans?

The EMS has previously been suggested to be one of the most oligotrophic marine systems on Earth, including a claim for the "deepest Secchi-depth world record" - 53 m during summertime (Berman et al. 1984). A comparison of published values of PP, including those measured in this study, supports this notion, with the median integrated PP being ~3-fold lower than Bermuda, the Red Sea and the Western Mediterranean Sea (WMS), and ~5-fold lower than station ALOHA (Figure 6A). Our estimates of PP during the SoMMoS cruises are among the lowest in the EMS (Figure 6A), yielding an annual PP of ~32 gC m^{-2} $year^{-1}$, although similar values have previously been reported (Dugdale and Wilkerson 1988). The annual PP during the SoMMoS cruises is approximately half of that reported above the continental slope of the Cretan Sea, ~59 gC m^{-2} y^{-1}, (Psarra et al. 2000), as well as in other more western locations in the EMS, ~62 gC m^{-2} y^{-1} (Boldrin et al. 2002). The values of integrated chlorophyll (Table 1, Figure 2A) and phytoplankton cell counts are also somewhat lower than previously-published measurements from the same region (Figure 4, Figure 7) (Berman et al. 1984; Robarts et al. 1996). Both the temperature and salinity minima during the SoMMoS cruise series were higher than the 2002-2020 climatological average (Herut and Rahav 2019), and thus we currently cannot determine whether the lower PP values measured during this annual cruise series are due to inter-annual variability, or whether these are due to technical aspects. Nevertheless, it is clear that the EMS is one of the most oligotrophic locations on Earth, as defined using primary production.

In addition to low PP, the EMS exhibits low sinking fluxes of particulate organic carbon (POC). The POC flux measured from the bottom of the photic layer (180 m) at the DeepLev mooring station, which is in the same region as the THEMO-2 site (Figure 1A, ~10Km north of our study site, Lat: 32.820 N; 34.380 E), is ~0.2 gC m^{-2} during the summer months (May-September 2018) and ~0.8 gC m^{-2} per year (Alkalay et al. 2020). This POC flux to the aphotic layer is less than 2% of the PP measured during summertime (~12 gC m^{-2} in 5 months) or 2.5% from the annual PP rates (~32 gC m^{-2} $year^{-1}$). The fraction of PP exported as particulate matter in the EMS is therefore lower than that reported in other oligotrophic systems; i.e., HOT and BATS stations ~5% (Karl and Church 2014; Steinberg et al. 2001). This low contribution provides an additional biogeochemical implication of the extreme oligotrophic conditions of the EMS. It also suggest that the dissolved organic carbon fraction derived from PP is likely rapidly recycled in the photic layer by heterotrophic/mixotrophic bacteria as often observed in LNLC environments, as reviewed in (Guyennon et al. 2015a; Santinelli 2015). We note, however, that estimates of new production based on nitrate+nitrate loss from the photic zone, calculated from the same data, are significantly higher (172 mmol N m^{-2} $year^{-1}$, corresponding to ~13.6g C m^{-2} $year^{-1}$, presented in a companion paper, Ben Ezra et al, *submitted*). The reason for this discrepancy is unclear, but may be due to over-estimation of new production (e.g. if part of the nitrate+nitrite was taken up by heterotrophic organisms) and/or under-estimation of the sinking carbon flux from sediment traps. Such an underestimation may be due to sinking flux from organisms too large to be caught in the sediment traps such as fish or jellyfish (Edelist et al. 2020; Lebrato et al. 2019).

In contrast to PP, integrated BP in the EMS was higher than estimates at BATS and HOT, and similar to the Red Sea (Figure 6B, which compares only measurements obtained using the ^{3}H-leucine incorporation method). Similar values were obtained in the South Pacific Gyre, 43-61 mg C m^{-2} d^{-1}, (Berman-Frank et al. 2016; Van Wambeke et al. 2008). Thus,

differences in PP between oligotrophic regions are not necessarily coupled to BP measurements. Previous studies, including from HOT and BATS, have shown that BP and PP are decoupled across multiple time-scales (e.g hours-months) (Carlson et al. 1996; Viviani and Church 2017). Similarly, PP and BP were uncoupled in the cyclonic Rhodes Gyre and the anti-cyclonic Cyprus Eddy of the EMS (Rahav et al. 2013b) and also in our study when BP increased in surface waters between June and November, while PP rates declined (Figure 3). One potential reason for this discrepancy is that PP is often measured on filtered samples (particulate PP), and thus does not include the fraction of dissolved organic carbon (DOC) fixed through PP that is released from the cells due to exudation or lysis (Viviani et al. 2015). When phytoplankton have sufficient carbon and light for photosynthesis yet nutrients such as P and N are limiting, photosynthesis is uncoupled from growth and high concentrations of DOC are often released to the environment (Berman-Frank and Dubinsky 1999). Previous studies from natural samples and from cultures of the numerically-dominant phytoplankton in the EMS, *Prochlorococcus* and *Synechococcus*, suggest a potentially high but variable fraction of released DOC (typically 20-70% of PP, with one study suggesting >90% in lab cultures, (Bertlisson et al. 2005; Dearth et al. 2019; López-Sandoval et al. 2013; Rosenberg et al. 2020; Thornton 2014; Viviani et al. 2015; Zhao et al. 2017). It is currently unclear whether autochthonous production (that is, local PP) is sufficient to support the growth requirements of heterotrophic bacteria, given what is known about the growth efficiency of bacteria. A study from the Cretan Sea suggesting that this is possible if the release of DOC from phytoplankton exceeds 40% of PP (Anderson and Turley 2003).

The EMS is affected by coastal intrusions of relatively chlorophyll-rich waters (Efrati et al. 2013), which could contribute also additional DOC, yet the importance of these processes in determining BP and PP requires additional studies, as they occur on temporal and spatial scales not captured by the SoMMoS cruise series. Such studies are also needed to understand

the relative contribution of dissolved compared to particulate carbon to export processes in oligotrophic regions (Guyennon et al. 2015b).

An additional explanation for the uncoupling between PP and BP was previously suggested following an *in-situ* phosphorus addition experiment at an anti-cyclonic eddy in the EMS, where orthophosphate addition led to chlorophyll *a* decrease while heterotrophic biomass and activity increased (Thingstad et al. 2005). The authors postulated two possible scenarios to explain their observation; 1) fast growing bacteria out-competed phytoplankton for the added phosphorus. Then, the accumulated heterotrophic biomass was quickly channeled toward larger consumers (the 'bypass hypothesis'). 2) luxury uptake of P, mainly by heterotrophic bacteria (and to a lesser extent by small-size picophytoplankton), formed a phosphorus-rich diet for grazers, resulting in increased egg production (the 'tunneling hypothesis'). Additionally, a scenario where an increase in temperature drives increased growth by heterotrophic bacteria (Apple et al. 2006; Luna et al. 2012), resulting in a draw-down of inorganic nutrients, could explain the increased BP in surface waters during summer, when no increase in PP was observed (Figure 3).

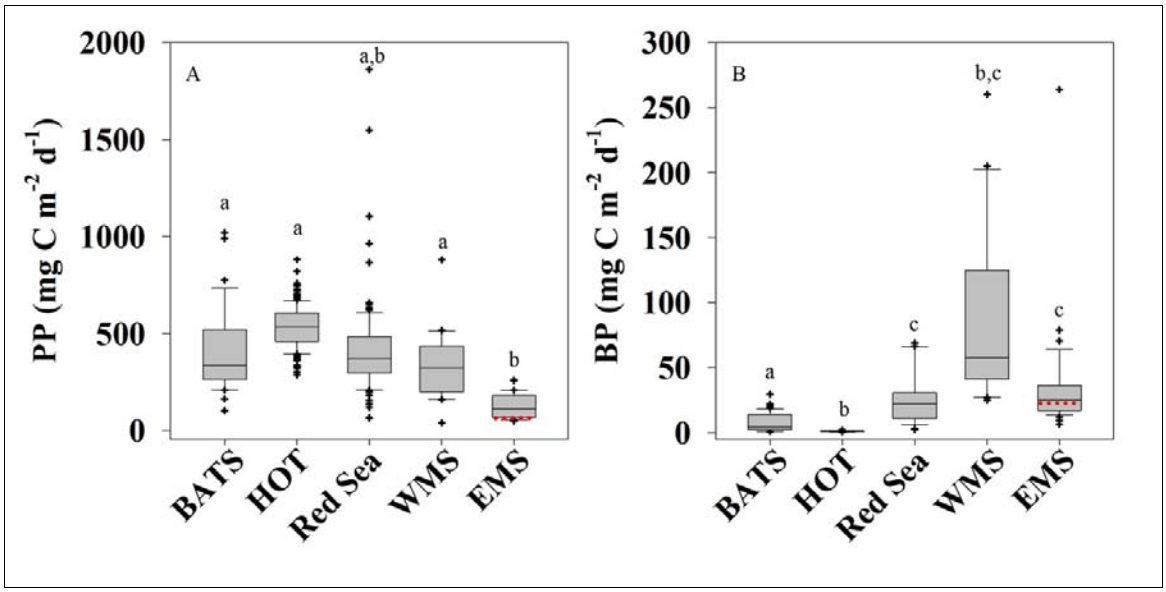

Figure 6: **Comparative literature analysis of the integrated primary and bacterial productivity** (PP and BP, respectively) in the EMS and other well-studied oligotrophic locations (Bianchi et al. 1999; Bonnet et al. 2011; Casotti et al. 2003; Christaki et al. 2011; Decembrini et al. 2009; Fernández et al. 1994; Gasol et al. 1998; Gaudy et al. 2003; Hazan et al. 2018; Ignatiades et al. 2002; Lemée et al. 2002; Lohrenz et al. 1988; Morán and Estrada 2001; Moutin and Raimbault 2002; Pedrós-Alió et al. 1999; Rahav et al. 2013b; Rahav et al. 2019; Robarts et al. 1996; Siokou-Frangou et al. 2002; Van Wambeke et al. 2004; Vidussi et al. 2000; Wambeke et al. 2002; Zervoudaki et al. 2007). Box-Whisker plots show the interquartile range (25th–75th percentile) of the data set. The horizontal line within the box represents the median value. The red dashed line in the EMS boxes shows the median values for the SoMMoS cruises described here. The letters above the box-plots represent significant differences (ANOVA, $p < 0.05$) for mean values between sampling sites. The BP compilation includes only measurements obtained using the ^{3}H-leucine incorporation method. Note the different Y axis.

4.2 What are the main phytoplankton in the EMS?

During the thermally mixed period, *Synechococcus* were more abundant than *Prochlorococcus* at the upper ~100 m (Figures 4). This period was characterized by measurable N at the surface while P concentrations were still extremely low – possibly causing P limitation (December-July, Table 1, Ben Ezra et al. *submitted*). In contrast, the extreme surface nutrient scarcity during the stratified period, when both N and P were below the limit of detection and were potentially co-limiting (Ben Ezra et al. submitted), likely contributed to the dominance of the small-size cyanobacterium *Prochlorococcus* over the somewhat larger-cell *Synechococcus* (Figures 4). It is generally accepted that, as the nutrient concentrations decrease (i.e., the water becomes more oligotrophic), so does the average size

of phytoplankton (Margalef and Kinne 1997). Additionally, while most *Synechococcus* genomes encode the genes required for nitrate uptake and utilization, this trait is found only in a subset of the *Prochlroococcus* genomes (Berube et al. 2019), and single-cell analysis suggests that more *Synechococcus* cells in nature utilize nitrate compared to *Prochlorococcus* (Berthelot et al. 2019). Thus, the type of nutrient limitation, P or N+P, (Krom et al. 1991; Tanaka et al. 2011; Thingstad et al. 2005; Zohary et al. 2005) may also affect the temporal dynamics of these two clades in the water column.

The abundances of these two cyanobacterial groups also differed with depth. *Synechococcus* was more abundant in the surface waters than *Prochlorococcus* (Fig 4). This was especially evident from May to September when *Prochlorococcus* cells could not be identified in the surface layer using either flow cytometry or pigment analysis (Figures 4 and 5, although this is likely due at least in part to the limit of detection of the methods used). It has been suggested that *Prochlorococcus'* unique photosynthetic pigments (DVChl-a and DVChl-b) provide a competitive advantage for these organisms at deeper layers of the water column, leading to a niche separation between these two pico-cyanobacteria (Moore et al. 1995). The observed niche (depth) separation between *Prochlorococcus* and *Synechococcus* has been previously observed including in the first description of *Prochlorococcus* from the North Atlantic and North Pacific (Chisholm et al. 1988), and the Eastern South Pacific (BIOSOPE cruise, (Huang et al. 2015; Zwirglmaier et al. 2008)). However, this is not a universal observation. At the HOT station in the North Pacific, *Prochlorococcus* and *Synechococcus* often show similar depth distributions, both being more abundant at the surface, with *Prochlorococcus* more abundant numerically and in terms of biomass (van den Engh et al. 2017). Similarly, in the Indian Ocean during May-June 2003 *Prochlorococcus* dominated the surface waters whereas *Synechococcus* were much less abundant (Huang et al. 2015; Zwirglmaier et al. 2008). Indeed, a global analysis of >35,000 quantitative measurements of

Prochlorococcus and *Synechococcus* found that *Prochlorococcus* were often more abundant than *Synechococcus* at high PAR and temperature values representative of surface waters in tropical waters (Flombaum et al. 2013). Thus, the reasons why *Prochlorococcus* and *Synechococcus* partitioned by both depth and season in the EMS, and why this is not necessarily observed elsewhere, remain unclear. Other factors probably also impact distribution, as was suggested for surface populations of *Prochlorococcus* that appeared to be negatively affected by atmospheric deposition through biological and chemical reactions (Rahav et al. 2020).

While the pico-cyanobacteria *Prochlorococcus* and *Synechococcus* were the most numerically abundant phytoplankton at THEMO-2, when biomass is examined the contribution of picoeukaryotes can be as high as that of the two pico-cyanobacteria, or even higher (Supplementary Figure S5, and see below). A previous study of the diversity of pico-phytoplankton in the EMS showed that pico-eukaryotes were not very common in terms of their DNA sequences or flow cytometry signals, but were often dominant in terms of RNA sequences, one potential proxy for photosynthetic activity (Man-Aharonovich et al. 2010). In that study, pico-eukaryotes were suggested to comprise up to 60% of the photosynthetic picoplankton biomass in surface waters, and were mainly composed of Haptophytes (primarily *Prymnesiophytes*) and *Stramenopiles* (Man-Aharonovich et al. 2010). In agreement with these observations, the photosynthetic pigment 19'-hexanoyloxyfucoxanthin (19'-hex), which is considered (together with 19'-butanoyloxyfucoxanthin, or 19'-but) to be a diagnostic pigment for *prymnesiophytes*, was found year-round in the water column, but was more abundant relative to the total phytoplankton biomass (i.e. in relation to total chlorophyll) during August-October (stratified period). Thus, both molecular evidence (Man-Aharonovich et al. 2010) and biochemical evidence (pigment analysis) point to the importance of prymnesiophytes in the EMS. A companion study from the SoMMoS cruises

provides an overview of seasonal dynamic and impact of calcified haptophytes (coccolithophores) during this yearly survey (Keuter et al, *in prep*).

Interestingly, we often observed 19'-hex around or below the DCM, including at depths where light intensities are very low and photosynthesis may not provide enough carbon or energy to support growth (Fig 5). Recent studies have unveiled that haptophytes, including coccolithophores, are mixotrophic - capable of acquiring prey by phagotrophy or organic compounds by osmotrophy in addition to photosynthesis (e.g. (Avrahami and Frada 2020; Godrijan et al. 2020; Tillmann 1998). Indeed, haptophytes can contribute to large fractions of total bacteriovory in marine settings (Frias-Lopez et al. 2009; Unrein et al. 2014). Further analysis of the DNA samples collected on the SoMMoS cruises may help identify mixotrophy within the phytoplankton clades found at the base of the photic layer (e.g. (Yelton et al. 2016) and help illuminate the metabolic capacities required to support phytoplankton growth in this environment.

Pigments associated with diatoms and dinoflagellates, which are often dominant phytoplankton groups (Andersen et al. 1996), were observed at relatively high concentrations only during January 2019 (Figure 5C, D). At this time DVChl-*a* measurement were below the detection limit in the water column, suggesting a succession from pico-cyanobacteria to larger eukaryotic organisms, which occurred relatively rapidly - over several weeks. This occurred concomitantly with a drop in surface temperature (Figure 2A) and thus a break in stratification, an increase in nitrate+nitrite (Ben Ezra et al. *submitted*), and a shift in coccolithophore population towards r-selected species such as *Emiliania huxleyi* which are indicative for a higher nutrient regime (Keuter et al, *in prep*). While chlorophyll-*a* concentrations increased both at the surface (including by satellite sensing, Figure 1B) and at the DCM (Figure 3A), no concomitant increase was measured in PP (Figure 3B). Yet, a major increase was observed in BP (Figure 3C). As described in detail in the materials and

methods, our measurements of PP likely underestimate productivity at depth, and the pigments were observed primarily below the mixed layer. It is possible that the phytoplankton bloom actually occurred several days before our cruise, and that the pigments observed are from stressed or dead phytoplankton. In this case, the major increase in BP observed at the time may represent heterotrophic bacteria utilizing dissolved and particulate organic carbon produced during the bloom.

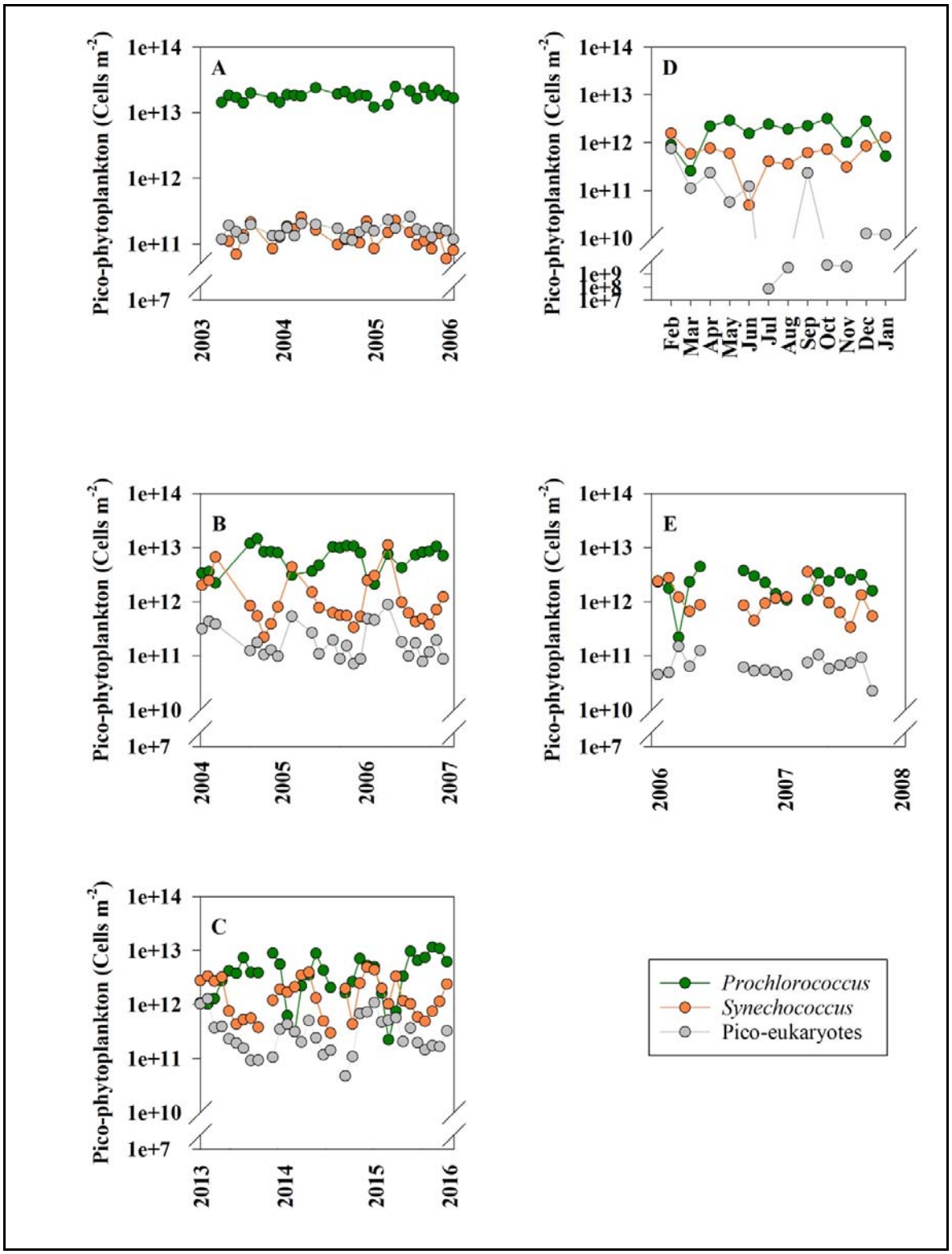
A
B
C
D
E
Pico-phytoplankton (Cells m-2)
1e+14
1e+13
1e+12
1e+11
1e+10
1e+9
1e+8
1e+7
2003
2004
2005
2006
2007
2008
2013
2014
2015
2016
Feb
Mar
Apr
May
Jun
Jul
Aug
Sep
Oct
Nov
Dec
Jan
Prochlorococcus
Synechococcus
Pico-eukaryotes

Figure 7: Integrated cell count time series of *Prochlorococcus* (green), *Synechococcus* (orange) and picoeukaryotes (gray) at stations HOT (A), BATS (B), the Northern Red Sea (C), and the EMS (D, E – this study and (Yogev et al. 2011) respectively). Abundance measurements were carried out using flow cytometry and are presented in a log scale. Data for stations HOT and BATS were compiled from (Malmstrom et al. 2010) and from the Northern Red Sea from the Eilat National Monitoring Program (Shaked and Genin 2017).

4.3 Phytoplankton composition and seasonality in the EMS in comparison to HOT, BATS and the Red Sea

The north Atlantic and Pacific gyres, the northern Red Sea and the EMS are all considered Low-Nutrient Low-Chlorophyll marine systems, with phytoplankton numerically dominated by pico-cyanobacteria throughout most of the year. Nevertheless, there are differences in the compositions and the seasonal dynamics of the different phytoplankton clades among these LNLC location (Fig. 7, Sup Fig. 5). Specifically, BATS, the Red Sea and the EMS all show seasonal succession patterns in the abundance of the main phytoplankton groups, although there are subtle differences between these sites: i) The period when integrated *Synechococcus* numbers are higher than *Prochlorococcus* is consistently longer in the Red Sea and EMS (3-4 months) compared to BATS (1-2 months); ii) *Prochlorococcus* reached higher absolute cell abundances during the stratified period at BATS (~10^{13} cells m^{-2}) compared to the Northern Red Sea or the EMS (~$2.5x10^{11}$ cells m^{-2}); iii) In terms of calculated biomass, the Red Sea is dominated by pico-eukaryotes for much of the year, whereas in BATS and the EMS the contribution of *Prochlorococcus*, *Synechococcus* and pico-eukaryotes to the total biomass is similar, and the dominant groups change over the year (Supporting Fig S5).

The absolute nutrient concentrations and the identity of the limiting nutrient(s) are different between these locations. For example, BATS is typically considered P limited, whereas the

EMS is potentially P limited during winter and co-limited by N and P during summer (Tsiola et al. 2016; Zohary et al. 2005)Ben-Ezra et al. *submitted*). There may also be differences in the length of the mixed period, its intensity, or the composition of the mixed water (e.g. deep water in the EMS have an N:P ratio of ~28:1, compared to the canonical 16:1 Redfield ratio of ~16:1, (Redfield 1934). Future work may use the observed differences in phytoplankton dynamics as a sensitive "readout" of the system, enabling a better understanding of the oceanographic processes underlying the differences between BATS, the Red Sea and the EMS.

In contrast to BATS, the Red Sea and the EMS, seasonality at HOT in is much less pronounced (Figure 7). *Prochlorococcus* are about 2-orders of magnitude more abundant than *Synechococcus* and pico-eukaryotes, and are also the most dominant in terms of biomass (Sup Fig. 5). The drivers of phytoplankton temporal dynamics at HOT are thus likely fundamentally different compared to BATS, the Red Sea and the EMS. It has been suggested that a-periodic events such as mesoscale eddies, Fe deposition from winds, and biological processes such as dinitrogen fixation, may be major drivers of phytoplankton dynamics at HOT (Karl and Church 2014; Letelier et al. 2019; Sohm et al. 2011) and less so in the EMS (Berman-Frank and Rahav 2012; Yogev et al. 2011).

5 Closing remarks

The year of data presented here show that the EMS is one of the most oligotrophic regions in the global oceans, as estimated based on PP (32 mg C m^{-2} year $^{-1}$), chlorophyll a (median ~10 mg m^{-2}), and dominance of small-size picophytoplankton with overall low abundances compared to other LNLC regions (in some cases ~2 orders of magnitude lower). In contrast, BP in the EMS is higher than at HOT and BATS, and similar to the Red and Western Mediterranean seas. This suggests that the system is overall heterotrophic, and that different

factors might limit phytoplankton and heterotrophic bacteria (e.g. (Thingstad et al. 2005). Despite these observations, there is a clear seasonal cycle in the phytoplankton populations and their activities, reminiscent of BATS and the Northern Red Sea (but not of HOT), suggesting that mixing (and potentially other seasonal processes such as dust deposition) drive similar processes across many, but not all, LNLC regions.

Our results also highlight important knowledge gaps regarding the EMS. For example, we do not know to what extent the bacterial populations or their physiological traits (e.g. bacterial carbon demand or growth efficiency) differ seasonally or vertically in the EMS, as well as compared to other LNLC locations. Detailed studies are also lacking of higher trophic levels in this region (dominant micro-grazer species, diversity, biomass, grazing rates, etc.). These are critical for understanding ecosystem dynamics including top-down vs. bottom-up regulations etc. Biogeochemical characterization of the EMS will also benefit from more explicit characterization of carbon-per-cell estimates, used to derive the biomass contributions from flow-cytometry counts (i.e. Supplementary Figure S5) can vary depending on taxonomy and physiological state (Campbell 2001; Kirchman 2012). Future studies of these aspects, together with other data emerging from the SoMMoS cruise series and the ocean observatories in the EMS, should provide the needed background for governments and other stakeholders to employ science-based environmental policies in this rapidly changing region.

Acknowledgements

We thank the captains and crew of the R/V Mediterranean Explorer (EcoOcean) and R/V Bat-Galim (IOLR), Oshra Yosef, Elad Rachmilovitz, Guy Sisma-Ventura for help with the sampling. The SoMMoS ship-time was funded by the Leon H. Charney School of Marine Sciences with help from EcoOcean and IOLR. This study was supported by grant RGP0020/2016 from the Human Frontiers Science Program (to DS), by grant number 1635070/2016532 from the NSF-BSF program in Oceanography (NSFOCE-BSF, to DS), and partly by the Israel Science Foundation (grants number 1211/17 to ER and BH and 996/08 to I. B-F and B.H). This study is in partial fulfilment of the M.Sc. thesis of Tom Reich (University of Haifa).

Author Contributions

MDK, YL, ER and DS initiated and designed study; TR, TBE, NB, DRR, OB, MDK, ER and DS collected samples; TR, TBE, NB and AT analyzed samples with help from MDK, DA, DRR and SG; TR, ER and DS wrote the manuscript with input from all co-authors.

References

Alkalay, R. and others 2020. Carbon export and drivers in the southeastern Levantine Basin. Deep Sea Research Part II: Topical Studies in Oceanography **171:** 104713.

Anabalón, V. and others 2016. Micro-phytoplankton community structure in the coastal upwelling zone off Concepción (central Chile): Annual and inter-annual fluctuations in a highly dynamic environment. Progress in Oceanography **149:** 174-188.

Andersen, R. A., R. R. Bidigare, M. D. Keller, and M. Latasa. 1996. A comparison of HPLC pigment signatures and electron microscopic observations for oligotrophic waters of the North Atlantic and Pacific Oceans. Deep Sea Research-Part II-Topical Studies in Oceanography **43:** 517-538.

Anderson, T. R., and C. M. Turley. 2003. Low bacterial growth efficiency in the oligotrophic eastern Mediterranean Sea: a modelling analysis. Journal of Plankton Research **25:** 1011-1019.

Apple, J. K., P. A. Del Giorgio, and W. M. Kemp. 2006. Temperature regulation of bacterial production, respiration, and growth efficiency in a temperate salt-marsh estuary. Aquatic Microbial Ecology **43:** 243-254.

Avnaim-Katav, S. and others 2020. Sediment trap and deep sea coretop sediments as tracers of recent changes in planktonic foraminifera assemblages in the southeastern ultra-oligotrophic Levantine Basin. Deep Sea Research Part II: Topical Studies in Oceanography **171:** 104669.

Avrahami, Y., and M. J. Frada. 2020. Detection of Phagotrophy in the Marine Phytoplankton Group of the Coccolithophores (Calcihaptophycidae, Haptophyta) During Nutrient-replete and Phosphate-limited Growth. Journal of phycology.

Azov, Y. 1986. Seasonal patterns of phytoplankton productivity and abundance in nearshore oligotrophic waters of the Levant Basin (Mediterranean). Journal of Plankton Research **8:** 41-53.

Behrenfeld, M. J. 2010. Abandoning Sverdrup's Critical Depth Hypothesis on phytoplankton blooms. Ecology **91:** 977-989.

Behrenfeld, M. J., and E. S. Boss. 2014. Resurrecting the ecological underpinnings of ocean plankton blooms.

Berman, T., D. Townsend, S. Elsayed, C. Trees, and Y. Azov. 1984. Optical transparency, chlorophyll and primary productivity in the Eastern Mediterranean near the Israeli coast. Oceanologica Acta **7:** 367-372.

Berman-Frank, I., and Z. Dubinsky. 1999. Balanced growth in aquatic plants: Myth or reality? Phytoplankton use the imbalance between carbon assimilation and biomass production to their strategic advantage. Bioscience **49:** 29-37.

Berman-Frank, I., and E. Rahav. 2012. Nitrogen fixation as a source for new production in the Mediterranean Sea: a review. Life in the Mediterranean Sea: A look at habitat changes**:** 199-226.

Berman-Frank, I., D. Spungin, E. Rahav, F. Van Wambeke, K. Turk-Kubo, and T. Moutin. 2016. Dynamics of transparent exopolymer particles (TEP) during the VAHINE mesocosm experiment in the New Caledonian lagoon. Biogeosciences **13**.

Berthelot, H. and others 2019. NanoSIMS single cell analyses reveal the contrasting nitrogen sources for small phytoplankton. The ISME journal **13:** 651-662.

Bertlisson, S., O. Berglund, M. J. Pullin, and S. W. Chisholm. 2005. Release of dissolved organic matter by Prochlorococcus. Vie et Milieu **55:** 225-232.

Berube, P. M., A. Rasmussen, R. Braakman, R. Stepanauskas, and S. W. Chisholm. 2019. Emergence of trait variability through the lens of nitrogen assimilation in.

Bianchi, F. and others 1999. Biogenic particulate matter and primary productivity in the Southern Adriatic and Northern Ionian seas, p. 120-121. 4th MTP-Workshop MATER., vol. Abstracts Volume.

Boldrin, A., S. Miserocchi, S. Rabitti, M. Turchetto, V. Balboni, and G. Socal. 2002. Particulate matter in the southern Adriatic and Ionian Sea: characterisation and downward fluxes. Journal of Marine Systems **33:** 389-410.

Bonnet, S., O. Grosso, and T. Moutin. 2011. Planktonic dinitrogen fixation along a longitudinal gradient across the Mediterranean Sea during the stratified period (BOUM cruise). Biogeosciences **8:** 2257-2267.

Brenner, S., Z. Rozentraub, J. Bishop, and M. Krom. 1991. The mixed-layer/thermocline cycle of a persistent warm core eddy in the eastern Mediterranean. Dynamics of Atmospheres and Oceans **15:** 457-476.

Campbell, L. 2001. Flow cytometric analysis of autotrophic picoplankton. Methods in microbiology **30:** 317-343.

Carlson, C. A., H. W. Ducklow, and T. D. Sleeter. 1996. Stocks and dynamics of bacterioplankton in the northwestern Sargasso Sea. Deep Sea Research Part II: Topical Studies in Oceanography **43:** 491-515.

Casotti, R. and others 2003. Composition and dynamics of the phytoplankton of the Ionian Sea (eastern Mediterranean). Journal of Geophysical Research: Oceans **108**.

Chisholm, S. W., R. J. Olson, E. R. Zettler, R. Goericke, J. B. Waterbury, and N. A. Welschmeyer. 1988. A novel free-living prochlorophyte abundant in the oceanic euphotic zone. Nature **334:** 340-343.

Christaki, U., A. Giannakourou, F. Van Wambeke, and G. Grégori. 2001. Nanoflagellate predation on auto-and heterotrophic picoplankton in the oligotrophic Mediterranean Sea. Journal of Plankton Research **23:** 1297-1310.

Christaki, U. and others 2011. Microbial food webs and metabolic state across oligotrophic waters of the Mediterranean Sea during summer. Biogeosciences **8:** 1839-1852.

d'Ortenzio, F. and others 2005. Seasonal variability of the mixed layer depth in the Mediterranean Sea as derived from in situ profiles. Geophysical Research Letters **32**.

Dearth, S. P., S. R. Campagna, and E. R. Zinser. 2019. Carbon Fate and Flux in Prochlorococcus under Nitrogen Limitation. MSystems **4**.

Decembrini, F., C. Caroppo, and M. Azzaro. 2009. Size structure and production of phytoplankton community and carbon pathways channelling in the Southern Tyrrhenian Sea (Western Mediterranean). Deep Sea Research Part II: Topical Studies in Oceanography **56:** 687-699.

Diamant, R., I. Shachar, Y. Makovsky, B. M. Ferreira, and N. A. Cruz. 2020. Cross-Sensor Quality Assurance for Marine Observatories. Remote Sensing **12:** 3470.

Dugdale, R. C., and F. P. Wilkerson. 1988. Nutrient sources and primary production in the Eastern Mediterranean. Oceanologica Acta, Special Issue.

Edelist, D., T. Guy-Haim, Z. Kuplik, N. Zuckerman, P. Nemoy, and D. L. Angel. 2020. Phenological shift in swarming patterns of Rhopilema nomadica in the Eastern Mediterranean Sea. Journal of Plankton Research **42:** 211-219.

Efrati, S. and others 2013. Intrusion of coastal waters into the pelagic eastern Mediterranean: in situ and satellite-based characterization. Biogeosciences **10:** 3349.

Fernández, M., M. Bianchi, and F. Van Wambeke. 1994. Bacterial biomass, heterotrophic production and utilization of dissolved organic matter photosynthetically produced in the Almeria-Oran front. Journal of Marine Systems **5:** 313-325.

Flombaum, P. and others 2013. Present and future global distributions of the marine Cyanobacteria Prochlorococcus and Synechococcus. Proc Natl Acad Sci U S A **110:** 9824-9829.

Frias-Lopez, J., A. Thompson, J. Waldbauer, and S. W. Chisholm. 2009. Use of stable isotope-labelled cells to identify active grazers of picocyanobacteria in ocean surface waters. Environmental microbiology **11:** 512-525.

Gasol, J. M. and others 1998. Diel variations in bacterial heterotrophic activity and growth in the northwestern Mediterranean Sea. Marine Ecology Progress Series **164:** 107-124.

Gaudy, R., F. Youssara, F. Diaz, and P. Raimbault. 2003. Biomass, metabolism and nutrition of zooplankton in the Gulf of Lions (NW Mediterranean). Oceanologica Acta **26:** 357-372.

Genin, A., M. Zarubin, and Y. Lindemann. 2018. Deep mixing, stratification and spring phytoplankton bloom in the northern Red Sea. 2018 Ocean Sciences Meeting. AGU.

Godrijan, J., D. Drapeau, and W. M. Balch. 2020. Mixotrophic uptake of organic compounds by coccolithophores. Limnology and oceanography **65:** 1410-1421.

Groom, S. and others 2005. Satellite-derived spatial and temporal biological variability in the Cyprus Eddy. Deep Sea Research Part II: Topical Studies in Oceanography **52:** 2990-3010.

Guieu, C. and others 2014. The significance of the episodic nature of atmospheric deposition to Low Nutrient Low Chlorophyll regions. Global Biogeochemical Cycles **28:** 1179-1198.

Gunn, K. L., L. M. Beal, S. Elipot, K. McMonigal, and A. Houk. 2020. Mixing of subtropical, central, and intermediate waters driven by shifting and pulsing of the Agulhas Current. Journal of Physical Oceanography **50:** 3545-3560.

Guyennon, A. and others 2015a. New insights into the organic carbon export in the Mediterranean Sea from 3-D modeling. Biogeosciences **12:** 7025-7046.

Guyennon, A. and others 2015b. New insights into the organic carbon export in the Mediterranean Sea from 3-D modeling.

Hazan, O. and others 2018. Mesopelagic Prokaryotes Alter Surface Phytoplankton Production during Simulated Deep Mixing Experiments in Eastern Mediterranean Sea Waters. Frontiers in Marine Science **5**.

Herut, B., and E. Rahav. 2019. The National Monitoring Program of Israel's Mediterranean waters – Scientific Report on Climate Change and Hydrography for 2018-2019.

Hooker, S. B. 2005. Second SeaWiFS HPLC analysis round-robin experiment (SeaHARRE-2). National Aeronautics and Space Administration, Goddard Space Flight Center.

Huang, S., S. Zhang, N. Jiao, and F. Chen. 2015. Marine cyanophages demonstrate biogeographic patterns throughout the global ocean. Applied and environmental microbiology **81:** 441-452.

Ignatiades, L. and others 2002. Phytoplankton size-based dynamics in the Aegean Sea (Eastern Mediterranean). Journal of Marine Systems **36:** 11-28.

Jickells, T. 1998. Nutrient biogeochemistry of the coastal zone. Science **281:** 217-222.

Karl, D. M., and M. J. Church. 2014. Microbial oceanography and the Hawaii Ocean Time-series programme. Nature Reviews Microbiology **12:** 699-713.

Katz, T. and others 2020. The first deep-sea mooring station in the eastern Levantine basin (DeepLev), outline and insights into regional sedimentological processes. Deep Sea Research Part II: Topical Studies in Oceanography **171:** 104663.

Kim, H., D. E. Lee, and H. W. Ducklow. 2019. Winter extratropical cyclones as a potential driver of a long-term decline of bacterial production in the Sargasso Sea near Bermuda. Geophysical Research Letters **46:** 5404-5412.

Kimor, B., and E. Wood. 1975. A plankton study in the eastern Mediterranean Sea. Marine Biology **29:** 321-333.

Kirchman, D. L. 2012. Degradation of organic material. Processes in microbial ecology. Oxford University Press Inc., New York, NY**:** 79-98.

Kress, N., I. Gertman, and B. Herut. 2014. Temporal evolution of physical and chemical characteristics of the water column in the Easternmost Levantine basin (Eastern Mediterranean Sea) from 2002 to 2010. Journal of Marine Systems **135:** 6-13.

Krom, M., N. Kress, I. Berman-Frank, and E. Rahav. 2014. Past, present and future patterns in the nutrient chemistry of the Eastern Mediterranean, p. 49-68. The Mediterranean Sea. Springer.

Krom, M., N. Kress, S. Brenner, and L. Gordon. 1991. Phosphorus limitation of primary productivity in the eastern Mediterranean Sea. Limnology and Oceanography **36:** 424-432.

Lebrato, M. and others 2019. Sinking of gelatinous zooplankton biomass increases deep carbon transfer efficiency globally. Global Biogeochemical Cycles **33:** 1764-1783.

Lemée, R., E. Rochelle-Newall, F. Van Wambeke, M.-D. Pizay, P. Rinaldi, and J.-P. Gattuso. 2002. Seasonal variation of bacterial production, respiration and growth efficiency in the open NW Mediterranean Sea. Aquatic Microbial Ecology **29:** 227-237.

Letelier, R. M. and others 2019. Climate-driven oscillation of phosphorus and iron limitation in the North Pacific Subtropical Gyre. Proceedings of the National Academy of Sciences **116:** 12720-12728.

Lohrenz, S. E., D. A. Wiesenburg, I. P. DePalma, K. S. Johnson, and D. E. Gustafson Jr. 1988. Interrelationships among primary production, chlorophyll, and environmental conditions in frontal regions of the western Mediterranean Sea. Deep Sea Research Part A. Oceanographic Research Papers **35:** 793-810.

López-Sandoval, D. C., T. Rodríguez-Ramos, P. Cermeño, and E. Marañón. 2013. Exudation of organic carbon by marine phytoplankton: dependence on taxon and cell size. Marine ecology progress series **477:** 53-60.

Luna, G., S. Bianchelli, F. Decembrini, E. De Domenico, R. Danovaro, and A. Dell'Anno. 2012. The dark portion of the Mediterranean Sea is a bioreactor of organic matter cycling. Global biogeochemical cycles **26**.

Malmstrom, R. R. and others 2010. Temporal dynamics of Prochlorococcus ecotypes in the Atlantic and Pacific oceans. ISME J **4:** 1252-1264.

Man-Aharonovich, D. and others 2010. Diversity of active marine picoeukaryotes in the Eastern Mediterranean Sea unveiled using photosystem-II psbA transcripts. ISME J **4:** 1044-1052.

Margalef, R., and O. Kinne. 1997. Excellence in Ecology. Germany: Ecology Institute.

Marty, J., and J. Chiavérini. 2010. Hydrological changes in the Ligurian Sea (NW Mediterranean, DYFAMED site) during 1995-2007 and biogeochemical consequences. Biogeosciences **7**.

Marty, J.-C., J. Chiavérini, M.-D. Pizay, and B. Avril. 2002. Seasonal and interannual dynamics of nutrients and phytoplankton pigments in the western Mediterranean Sea at the DYFAMED time-series station (1991–1999). Deep Sea Research Part II: Topical Studies in Oceanography **49:** 1965-1985.

Mena, C. and others 2019. Phytoplankton Community Structure Is Driven by Stratification in the Oligotrophic Mediterranean Sea. Front Microbiol **10:** 1698.

Moore, L. R., R. Goericke, and S. W. Chisholm. 1995. Comparative physiology of Synechococcus and Prochlorococcus: influence of light and temperature on growth, pigments, fluorescence and absorptive properties. Marine Ecology Progress Series**:** 259-275.

Morán, X. A. G., and M. Estrada. 2001. Short-term variability of photosynthetic parameters and particulate and dissolved primary production in the Alboran Sea (SW Mediterranean). Marine Ecology Progress Series **212:** 53-67.

Moutin, T., and P. Raimbault. 2002. Primary production, carbon export and nutrients availability in western and eastern Mediterranean Sea in early summer 1996 (MINOS cruise). Journal of marine systems **33:** 273-288.

Nielsen, E. S. 1952. The use of radio-active carbon (C14) for measuring organic production in the sea. ICES Journal of Marine Science **18:** 117-140.

Ozer, T., I. Gertman, N. Kress, J. Silverman, and B. Herut. 2017. Interannual thermohaline (1979–2014) and nutrient (2002–2014) dynamics in the Levantine surface and intermediate water masses, SE Mediterranean Sea. Global and Planetary Change **151:** 60-67.

Pedrós-Alió, C., J.-I. Calderón-Paz, N. Guixa-Boixereu, M. Estrada, and J. M. Gasol. 1999. Bacterioplankton and phytoplankton biomass and production during summer stratification in the northwestern Mediterranean Sea. Deep Sea Research Part I: Oceanographic Research Papers **46:** 985-1019.

Peled, Y., S. Z. Shamir, M. Shechter, E. Rahav, and A. Israel. 2018. A new perspective on valuating marine climate regulation: The Israeli Mediterranean as a case study. Ecosystem Services **29:** 83-90.

Pinardi, N., and E. Masetti. 2000. Variability of the large scale general circulation of the Mediterranean Sea from observations and modelling: a review. Palaeogeography, Palaeoclimatology, Palaeoecology **158:** 153-173.

Psarra, S., A. Tselepides, and L. Ignatiades. 2000. Primary productivity in the oligotrophic Cretan Sea (NE Mediterranean): seasonal and interannual variability. Progress in Oceanography **46:** 187-204.

Rahav, E., N. Belkin, A. Paytan, and B. Herut. 2018. Phytoplankton and bacterial response to desert dust deposition in the coastal waters of the Southeastern Mediterranean Sea: A four-year in situ survey. Atmosphere **9:** 305.

Rahav, E., B. Herut, A. Levi, M. Mulholland, and I. Berman-Frank. 2013a. Springtime contribution of dinitrogen fixation to primary production across the Mediterranean Sea. Ocean Science **9:** 489-498.

Rahav, E., B. Herut, N. Stambler, E. Bar-Zeev, M. R. Mulholland, and I. Berman-Frank. 2013b. Uncoupling between dinitrogen fixation and primary productivity in the eastern Mediterranean Sea. Journal of Geophysical Research: Biogeosciences **118:** 195-202.

Rahav, E. and others 2020. Bio-Aerosols Negatively Affect Prochlorococcus in Oligotrophic Aerosol-Rich Marine Regions. Atmosphere **11:** 540.

Rahav, E. and others 2019. The deep water of Eastern Mediterranean Sea is a hotspot for bacterial activity. Deep Sea Research Part II: Topical Studies in Oceanography **164:** 135-143.

Raveh, O., N. David, G. Rilov, and E. Rahav. 2015. The Temporal Dynamics of Coastal Phytoplankton and Bacterioplankton in the Eastern Mediterranean Sea. PLoS One **10:** e0140690.

Redfield, A. C. 1934. On the proportions of organic derivatives in sea water and their relation to the composition of plankton. University Press of Liverpool Liverpool.

Robarts, R. D., T. Zohary, M. J. Waiser, and Y. Yacobi. 1996. Bacterial abundance, biomass, and production in relation to phytoplankton biomass in the Levantine Basin of the southeastern Mediterranean Sea. Marine ecology progress series **137:** 273-281.

Rosenberg, D. R. and others 2020. Particle-associated and free-living bacterial communities in an oligotrophic sea are affected by different environmental and anthropogenic factors. bioRxiv**:** 2020.2004.2020.051391.

Santinelli, C. 2015. DOC in the Mediterranean Sea, p. 579-608. Biogeochemistry of marine dissolved organic matter. Elsevier.

Shaked, Y., and A. Genin. 2017. Eilat IUI monitoring NMP Report 2017.

Signorini, S. R., B. A. Franz, and C. R. McClain. 2015. Chlorophyll variability in the oligotrophic gyres: mechanisms, seasonality and trends. Frontiers in Marine Science **2**.

Simon, M., and F. Azam. 1989. Protein content and protein synthesis rates of planktonic marine bacteria. Marine ecology progress series. Oldendorf **51:** 201-213.

Siokou-Frangou, I. and others 2002. Carbon flow in the planktonic food web along a gradient of oligotrophy in the Aegean Sea (Mediterranean Sea). Journal of Marine Systems **33:** 335-353.

Siokou-Frangou, I. and others 2010. Plankton in the open Mediterranean Sea: a review. Biogeosciences **7:** 1543-1586.

Sisma-Ventura, G. and others 2021. Post-eastern Mediterranean transient oxygen decline in the deep waters of the southeast Mediterranean Sea supports weakening of ventilation rate. Front Mar Sci **7:** 598686.

Smith, D. C., and F. Azam. 1992. A simple, economical method for measuring bacterial protein synthesis rates in seawater using 3H-leucine. Mar. Microb. food webs **6:** 107-114.

Sohm, J. A., E. A. Webb, and D. G. Capone. 2011. Emerging patterns of marine nitrogen fixation. Nature Reviews Microbiology **9:** 499-508.

Steinberg, D. K., C. A. Carlson, N. R. Bates, R. J. Johnson, A. F. Michaels, and A. H. Knap. 2001. Overview of the US JGOFS Bermuda Atlantic Time-series Study (BATS): a decade-scale look at ocean biology and biogeochemistry. Deep Sea Research Part II: Topical Studies in Oceanography **48:** 1405-1447.

Tanaka, T. and others 2011. Lack of P-limitation of phytoplankton and heterotrophic prokaryotes in surface waters of three anticyclonic eddies in the stratified Mediterranean Sea. Biogeosciences **8:** 525-538.

Tanaka, T. and others 2007. Microbial community structure and function in the Levantine Basin of the eastern Mediterranean. Deep Sea Research Part I: Oceanographic Research Papers **54:** 1721-1743.

Tanhua, T., D. Hainbucher, K. Schroeder, V. Cardin, M. Álvarez, and G. Civitarese. 2013. The Mediterranean Sea system: a review and an introduction to the special issue. Ocean Science **9:** 789-803.

Thingstad, T. F. and others 2005. Nature of phosphorus limitation in the ultraoligotrophic eastern Mediterranean. Science **309:** 1068-1071.

Thornton, D. C. 2014. Dissolved organic matter (DOM) release by phytoplankton in the contemporary and future ocean. European Journal of Phycology **49:** 20-46.

Tillmann, U. 1998. Phagotrophy by a plastidic haptophyte, Prymnesium patelliferum. Aquatic Microbial Ecology **14:** 155-160.

Tsiola, A. and others 2016. Nutrient limitation in surface waters of the oligotrophic Eastern Mediterranean Sea: an Enrichment Microcosm Experiment. Microbial ecology **71:** 575-588.

Unrein, F., J. M. Gasol, F. Not, I. Forn, and R. Massana. 2014. Mixotrophic haptophytes are key bacterial grazers in oligotrophic coastal waters. The ISME journal **8:** 164-176.

van den Engh, G. J., J. K. Doggett, A. W. Thompson, M. A. Doblin, C. N. Gimpel, and D. M. Karl. 2017. Dynamics of prochlorococcus and synechococcus at station ALOHA revealed through flow cytometry and high-resolution vertical sampling. Frontiers in Marine Science **4:** 359.

Van Wambeke, F., U. Christaki, M. Bianchi, S. Psarra, and A. Tselepides. 2000. Heterotrophic bacterial production in the Cretan Sea (NE Mediterranean). Progress in Oceanography **46:** 205-216.

Van Wambeke, F. and others 2004. Distribution of microbial biomass, production, respiration, dissolved organic carbon and factors controlling bacterial production across a geostrophic front (Almeria-Oran, SW Mediterranean Sea). Marine Ecology Progress Series **269:** 1-15.

Van Wambeke, F., I. Obernosterer, T. Moutin, S. Duhamel, O. Ulloa, and H. Claustre. 2008. Heterotrophic bacterial production in the eastern South Pacific: longitudinal trends and coupling with primary production.

Vidussi, F., J.-C. Marty, and J. Chiavérini. 2000. Phytoplankton pigment variations during the transition from spring bloom to oligotrophy in the northwestern Mediterranean Sea. Deep Sea Research Part I: Oceanographic Research Papers **47:** 423-445.

Viviani, D. A., and M. J. Church. 2017. Decoupling between bacterial production and primary production over multiple time scales in the North Pacific Subtropical Gyre. Deep Sea Research Part I: Oceanographic Research Papers **121:** 132-142.

Viviani, D. A., D. M. Karl, and M. J. Church. 2015. Variability in photosynthetic production of dissolved and particulate organic carbon in the North Pacific Subtropical Gyre. Frontiers in Marine Science **2:** 73.

Wambeke, F., U. Christaki, A. Giannakourou, T. Moutin, and K. Souvemerzoglou. 2002. Longitudinal and vertical trends of bacterial limitation by phosphorus and carbon in the Mediterranean Sea. Microbial ecology **43:** 119-133.

Williams, P. J. l. B., P. D. Quay, T. K. Westberry, and M. J. Behrenfeld. 2013. The oligotrophic ocean is autotrophic. Annual review of marine science **5:** 535-549.

Yacobi, Y. and others 1995. Chlorophyll distribution throughout the southeastern Mediterranean in relation to the physical structure of the water mass. Journal of Marine Systems **6:** 179-190.

Yelton, A. P., S. G. Acinas, S. Sunagawa, P. Bork, C. Pedrós-Alió, and S. W. Chisholm. 2016. Global genetic capacity for mixotrophy in marine picocyanobacteria. The ISME journal **10:** 2946-2957.

Yogev, T. and others 2011. Is dinitrogen fixation significant in the Levantine Basin, east Mediterranean Sea? Environmental microbiology **13:** 854-871.

Zervakis, V., and D. Georgopoulos. 2002. Hydrology and circulation in the North Aegean (eastern Mediterranean) throughout 1997 and 1998. Mediterranean Marine Science **3:** 5-19.

Zervoudaki, S. and others 2007. The importance of small-sized copepods in a frontal area of the Aegean Sea. Journal of Plankton Research **29:** 317-338.

Zhao, Z. and others 2017. Picocyanobacteria and deep-ocean fluorescent dissolved organic matter share similar optical properties. Nature communications **8:** 15284.

Zohary, T. and others 2005. P-limited bacteria but N and P co-limited phytoplankton in the Eastern Mediterranean—a microcosm experiment. Deep Sea Research Part II: Topical Studies in Oceanography **52:** 3011-3023.

Zwirglmaier, K. and others 2008. Global phylogeography of marine Synechococcus and Prochlorococcus reveals a distinct partitioning of lineages among oceanic biomes. Environmental microbiology **10:** 147-161.